

<sup>1</sup> The human visual system preserves the hierarchy  
<sup>2</sup> of 2-dimensional pattern regularity

<sup>3</sup> Peter J. Kohler<sup>1,2,3</sup> and Alasdair D. F. Clarke<sup>4</sup>

<sup>4</sup> *<sup>1</sup> York University, Department of Psychology, Toronto, ON M3J 1P3, Canada*

<sup>5</sup> *<sup>2</sup> Centre for Vision Research, York University, Toronto, ON, M3J 1P3, Canada*

<sup>6</sup> *<sup>3</sup> Stanford University, Department of Psychology, Stanford, CA 94305, United States*

<sup>7</sup> *<sup>4</sup> University of Essex, Department of Psychology, Colchester, UK, CO4 3SQ*

<sup>8</sup> **Abstract**

Symmetries are present at many scales in natural scenes. Humans and other animals are highly sensitive to visual symmetry, and symmetry contributes to numerous domains of visual perception. The four fundamental symmetries, reflection, rotation, translation and glide reflection, can be combined into exactly 17 distinct regular textures. These *wallpaper groups* represent the complete set of symmetries in 2D images. The current study seeks to provide a more comprehensive description of responses to symmetry in the human visual system, by collecting both brain imaging (Steady-State Visual Evoked Potentials measured using high-density EEG) and behavioral (symmetry detection thresholds) data using the entire set of wallpaper groups. This allows us to probe the hierarchy of complexity among wallpaper groups, in which simpler groups are subgroups of more complex ones. We find that both behavior and brain activity preserve the hierarchy almost perfectly: Subgroups consistently produce lower amplitude symmetry-specific responses in visual cortex and require longer presentation durations to be reliably detected. These findings expand our understanding of symmetry perception by showing that the human brain encodes symmetries with a high level of precision and detail. This opens new avenues for research on how fine-grained representations of regular textures contribute to natural vision.

Symmetries are abundant in natural and man-made environments, due to a complex interplay of physical forces that govern pattern formation in nature. Sensitivity to symmetry has been demonstrated in a number of species, includes bees (Giurfa et al., 1996), fish (Morris and Casey, 1998; Schlüter et al., 1998), birds (Møller, 1992; Swaddle and Cuthill, 1994) and dolphins (von Fersen et al., 1992), and may be used as a cue for mate selection in many species (Swaddle, 1999) including humans (Rhodes et al., 1998). Humans cultures have created and appreciated symmetrical patterns throughout history, and since the gestalt movement of the early 20th century, symmetry has been recognized as important for visual perception. Symmetry contributes to the perception of shapes (Palmer, 1985; Li et al., 2013), scenes (Apthorp and Bell, 2015) and surface properties (Cohen and Zaidi, 2013). This literature is almost exclusively based on stimuli in which one or more symmetry axes are placed at a single point in the image. Focus has been on mirror symmetry or *reflection*, with relatively few studies including the other fundamental

37 symmetries: *rotation*, *translation* and *glide reflection* (Wagemans, 1998) - perhaps because reflection  
38 has been found to be more perceptually salient (Mach, 1959; Royer, 1981; Palmer, 1991; Ogden  
39 et al., 2016; Hamada and Ishihara, 1988) and produce more brain activity (Makin et al., 2013, 2014,  
40 2012; Wright et al., 2015). In the current study, we take a different approach by investigating  
41 visual processing of regular textures in which combinations of the four fundamental symmetries  
42 tile the 2D plane.

43 In the two spatial dimensions relevant for images, symmetries can be combined in 17 distinct  
44 ways, *the wallpaper groups* (Fedorov, 1891; Polya, 1924; Liu et al., 2010). Previous work on a subset  
45 of four of the wallpaper groups used functional MRI to demonstrate that rotation symmetries  
46 in wallpapers elicit parametric responses in several areas in occipital cortex, beginning with  
47 visual area V3 (Kohler et al., 2016). This effect was also robust when symmetry responses were  
48 measured with electroencephalography (EEG) using both Steady-State Visual Evoked Potentials  
49 (SSVEPs)(Kohler et al., 2016) and Event-Related Potentials (Kohler et al., 2018). The SSVEP  
50 technique uses periodic visual stimulation to produce a periodic brain response that is confined to  
51 integer multiples of the stimulation frequency known as harmonics. SSVEP response harmonics  
52 can be isolated in the frequency domain and depending on the specific design, different harmonics  
53 will express different aspects of the brain response. (Norcia et al., 2015). Here we extend on the  
54 previous work by collecting SSVEPs and psychophysical data from human participants viewing  
55 the full set of wallpaper groups. We measure responses in visual cortex to 16 out of the 17  
56 wallpaper groups, with the 17th serving as a control stimulus. Our goal is to provide a more  
57 complete picture of how wallpaper groups are represented in the human visual system.

58 A wallpaper group is a topologically discrete group of isometries of the Euclidean plane, i.e.  
59 transformations that preserve distance (Liu et al., 2010). The wallpaper groups differ in the  
60 number and kind of these transformations and we can uniquely refer to different groups using  
61 crystallographic notation. In brief, most groups are notated by  $PXZ$ , where  $X \in \{1, 2, 3, 4, 6\}$   
62 indicates the highest order of rotation symmetry and  $Z \in \{m, g\}$  indicates whether the pattern  
63 contains reflection (m) or glide reflection (g). For example,  $P4$  contains rotation of order 4, while  
64  $P4MM$  contains rotation of order 4 and two reflections. By convention, many of the groups  
65 are given shortened names: for example,  $P4MM$  is usually referred to as  $P4M$ , as the second  
66 reflection can be deduced from the presence of rotation of order 4 alongside a reflection. Two of  
67 the groups start with a  $C$  rather than a  $P$ , ( $CM$  and  $CMM$ ) which indicates that the symmetries  
68 are specified relative to a cell that itself contains repetition. Full details of the naming convention  
69 can be found on [wikipedia](#) and examples of the wallpaper groups are shown in Figures 1 and 2.

70 In mathematical group theory, when the elements of one group is completely contained in  
71 another, the inner group is called a subgroup of the outer group (Liu et al., 2010). The full list  
72 of subgroup relationships is listed in Section 1.4.2 of the Supplementary Material. Subgroup  
73 relationships between wallpaper groups can be distinguished by their indices. The index of a  
74 subgroup relationship is the number of cosets, i.e. the number of times the subgroup is found  
75 in the supergroup (Liu et al., 2010). As an example, let us consider groups  $P_2$  and  $P_6$  (see Figure  
76 1B). If we ignore the translations in two directions that both groups share, group  $P_6$  consists  
77 of the set of rotations  $\{0^\circ, 60^\circ, 120^\circ, 180^\circ, 240^\circ, 300^\circ\}$ , in which  $P_2 \{0^\circ, 180^\circ\}$  is contained.  $P_2$

is thus a subgroup of  $P_6$ , and  $P_6$  can be generated by combining  $P_2$  with rotations  $\{0^\circ, 120^\circ, 240^\circ\}$ . Because  $P_2$  is repeated three times in  $P_6$ ,  $P_2$  is a subgroup of  $P_6$  with index 3 (Liu et al., 2010). Similarly,  $PMM$  contains two reflections and rotations  $\{0^\circ, 180^\circ\}$ .  $PMM$  can be generated by adding an additional reflection to both  $P_2$  ( $\{0^\circ, 180^\circ\}$ ) and  $PM$  (one reflection), so  $P_2$  and  $PM$  are both subgroups of  $PMM$  with index 2 (see Figure 1C). The 17 wallpaper groups thus obey a hierarchy of complexity where simpler groups are subgroups of more complex ones (Coxeter and Moser, 1972).

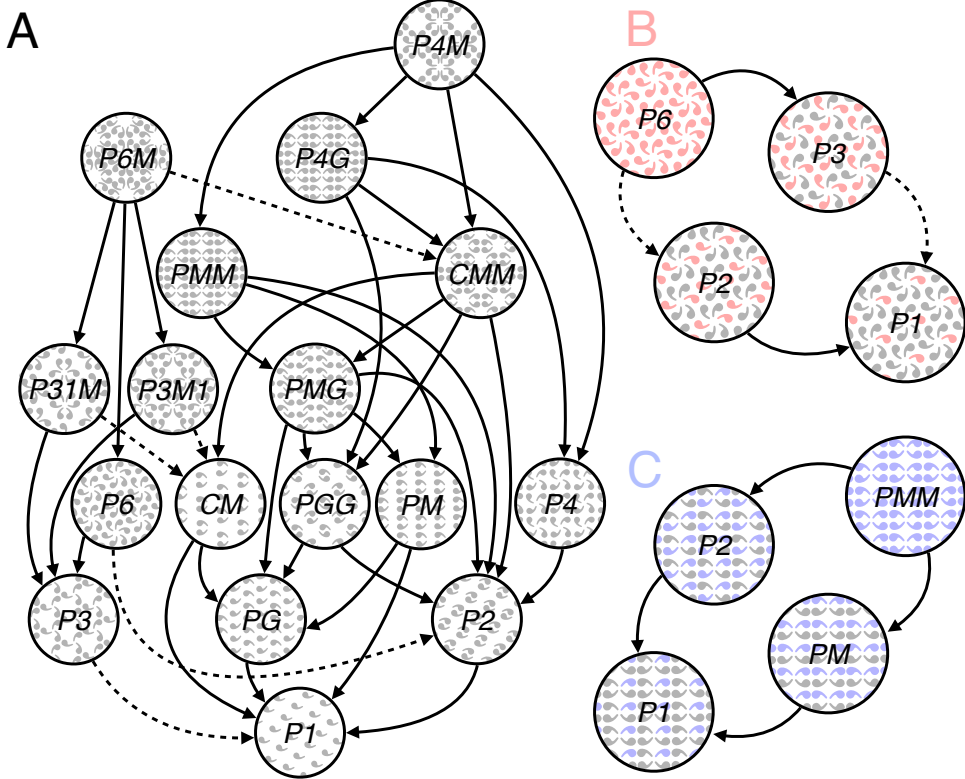


Figure 1: Subgroup relationships with indices 2 (solid lines) and 3 (dashed line) are shown in (A). All other relationships can be inferred by identifying the shortest path through the hierarchy, and multiplying the subgroup indices. For example,  $P_1$  is related to  $P_6$  through  $P_6 \rightarrow P_3$  (index 2) and  $P_3 \rightarrow P_1$  (index 3) so  $P_1$  is also a subgroup of  $P_6$  with index  $3 \times 2 = 6$ . We also show enlarged versions of some of the subgroup relationships involving  $P_6$  (B, shown in red) and  $PMM$  (C, shown in blue) and highlight the symmetries within the subgroups to emphasize how the supergroup can be generated by adding additional transformations to the subgroup.

The two datasets we present here make it possible to assess the extent to which both behavior and brain responses follow the hierarchy of complexity expressed by the subgroup relationships. Based on previous brain imaging work showing that patterns with more axes of symmetry produce greater activity in visual cortex (Sasaki et al., 2005; Tyler et al., 2005; Kohler et al., 2018, 2016; Keefe et al., 2018), we hypothesized that more complex groups would produce larger SSVEPs. For the psychophysical data, we hypothesized that more complex groups would lead to shorter symmetry detection thresholds, based on previous data showing that under a fixed presentation time, discriminability increases with the number of symmetry axes in the pattern (Wagemans et al., 1991). Our results confirm both hypotheses, and show that activity in human visual cortex

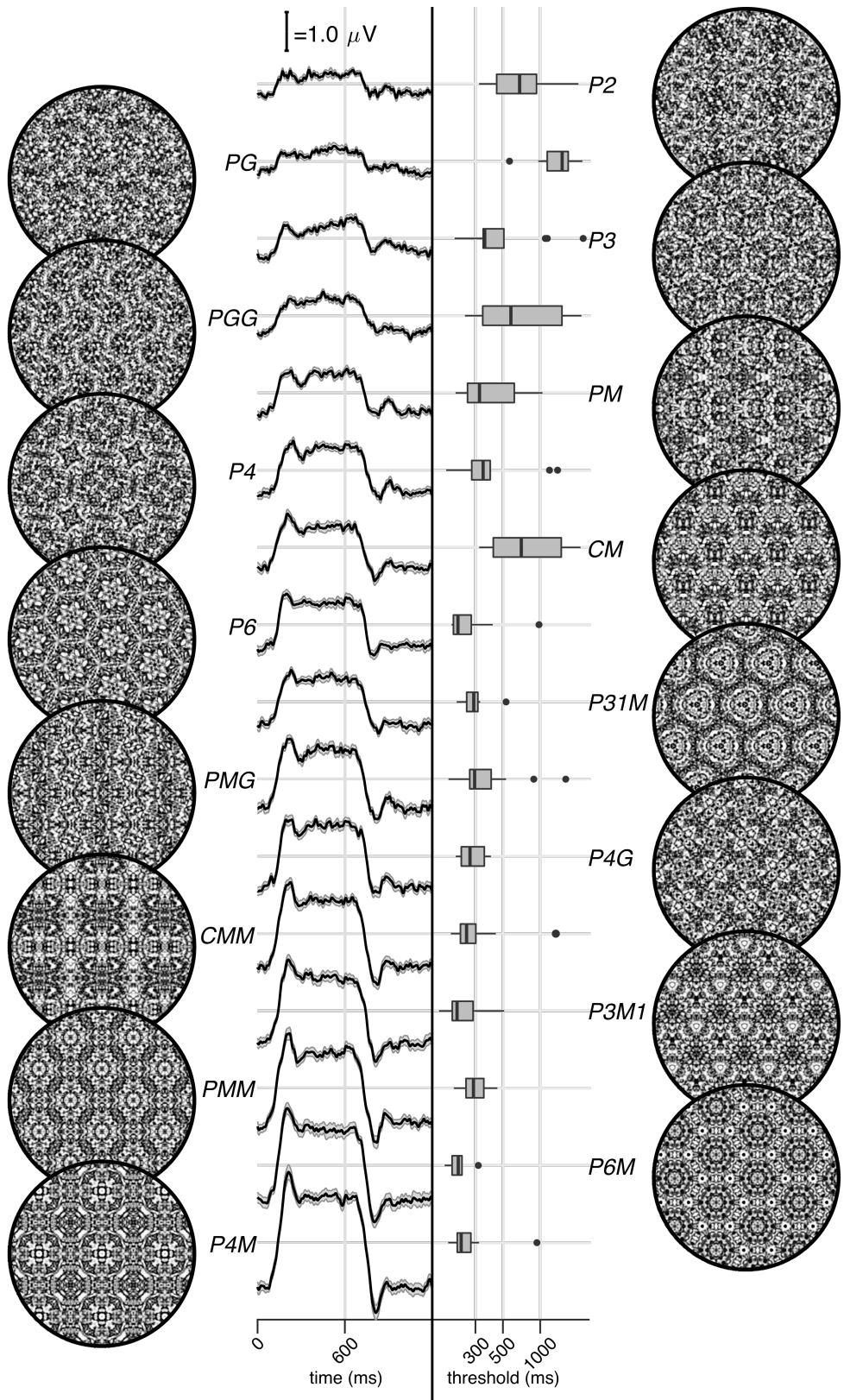


Figure 2: Examples of each of the 16 wallpaper groups are shown in the left- and right-most column of the figures, next to the corresponding SSVEP (center-left) and psychological (center-right) data from each group. The SSVEP data are odd-harmonic-filtered cycle-average waveforms. In each cycle, a  $P_1$  exemplar was shown for the first 600 ms, followed by the original exemplar for the last 600 ms. Errorbars are standard error of the mean. Psychophysical data are presented as boxplots reflecting the distribution of display duration thresholds. The 16 groups are ordered by the strength of the SSVEP response, to highlight the range of response amplitudes.

is remarkably consistent with the hierarchical relationships between the wallpaper groups, with SSVEP amplitudes and psychophysical thresholds following these relationships at a level that is far beyond chance. The human visual system thus appears to encode all of the fundamental symmetries using a representational structure that closely approximates the subgroup relationships from group theory.

## Results

The stimuli used in our two experiments were generated from random-noise textures, which made it possible to generate multiple exemplars from each of the wallpaper groups, as described in detail elsewhere (Kohler et al., 2016). We generated control stimuli matched to each exemplar in the main stimulus set, by scrambling the phase but maintaining the power spectrum. All wallpaper groups are inherently periodic because of their repeating lattice structure. Phase scrambling maintains this periodicity, so the phase-scrambled control images all belong to group  $P_1$  regardless of group membership of the original exemplar.  $P_1$  contains no symmetries other than translation, while all other groups contain translation in combination with one or more of the other three fundamental symmetries (reflection, rotation, glide reflection) (Liu et al., 2010). In our SSVEP experiment, this stimulus set allowed us to isolate brain activity specific to the symmetry structure in the exemplar images from activity associated with modulation of low-level features, by alternating exemplar images and control exemplars. In this design, responses to structural features beyond the shared power spectrum, including any symmetries other than translation, are isolated in the odd harmonics of the image update frequency (Kohler et al., 2016; Norcia et al., 2015, 2002). Thus, the combined magnitude of the odd harmonic response components can be used as a measure of the overall strength of the visual cortex response.

The psychophysical experiment took a distinct but related approach. In each trial an exemplar image was shown with its matched control, one image after the other, and the order varied pseudorandomly such that in half the trials the original exemplar was shown first, and in the other half the control image was shown first. After each trial, participants were instructed to indicate whether the first or second image contained more structure. The duration of both images was controlled by a staircase procedure so that a threshold duration for symmetry detection could be computed for each wallpaper group.

Examples of the wallpaper groups and a summary of our brain imaging and psychophysical measurements are shown in Figure 2. For our primary SSVEP analysis, we only considered EEG data from a pre-determined region-of-interest (ROI) consisting of six electrodes over occipital cortex (see Supplementary Figure 1.1). SSVEP data from this ROI was filtered so that only the odd harmonics that capture the symmetry response contribute to the waveforms. While waveform amplitude is quite variable among the 16 groups, all groups have a sustained negative-going response that begins at about the same time for all groups, 180 ms after the transition from the  $P_1$  control exemplar to the original exemplar. To reduce the amplitude of the symmetry-specific response to a single number that could be used in further analyses and compared to the psychophysical data, we computed the root-mean-square (RMS) over the odd-harmonic-filtered waveforms. The data

in Figure 2 are shown in descending order according to RMS. The psychophysical results, shown in box plots in Figure 2, were also quite variable between groups, and there seems to be a general pattern where wallpaper groups near the top of the figure, that have lower SSVEP amplitudes, also have longer psychophysical threshold durations.

We now wanted to test our two hypotheses about how SSVEP amplitudes and threshold durations would follow subgroup relationships, and thereby quantify the degree to which our two measurements were consistent with the group theoretical hierarchy of complexity. We tested each hypothesis using the same approach. We first fitted a Bayesian model with wallpaper group as a factor and participant as a random effect. We fit the model separately for SSVEP RMS and psychophysical data and then computed posterior distributions for the difference between supergroup and subgroup. These difference distributions allowed us to compute the conditional probability that the supergroup would produce (a) larger RMS and (b) a shorter threshold durations, when compared to the subgroup. The posterior distributions are shown in Figure 3 for the SSVEP data, and in Figure 4 for the psychophysical data, which distributions color-coded according to conditional probability. For both data sets our hypothesis is confirmed: For the overwhelming majority of the 63 subgroup relationships, supergroups are more likely to produce larger symmetry-specific SSVEPs and shorter symmetry detection threshold durations, and in most cases the conditional probability of this happening is extremely high.

We also ran a control analysis using (1) odd-harmonic SSVEP data from a six-electrode ROI over parietal cortex (see Supplementary Figure 1.1) and (2) even-harmonic SSVEP data from the same occipital ROI that was used in our primary analysis. By comparing these two control analysis to our primary SSVEP analysis, we can address the specify of our effects in terms of location (occipital cortex vs parietal cortex) and harmonic (odd vs even). For both control analyses (plotted in Supplementary Figures 3.3 and 3.4), the correspondence between data and subgroup relationships was substantially weaker than in the primary analysis. We can quantify the strength of the association between the data and the subgroup relationships, by asking what proportion of subgroup relationships that reach or exceed a range of probability thresholds. This is plotted in Figure 5, for our psychophysical data, our primary SSVEP analysis and our two control SSVEP analyses. It shows that odd-harmonic SSVEP data from the occipital ROI and symmetry detection threshold durations both have a strong association with the subgroup relationships such that a clear majority of the subgroups survive even at the highest threshold we consider ( $p(\Delta > 0 | data) > 0.99$ ). The association is far weaker for the two control analyses.

SSVEP data from four of the wallpaper groups ( $P_2$ ,  $P_3$ ,  $P_4$  and  $P_6$ ) was previously published as part of our earlier demonstration of parametric responses to rotation symmetry in wallpaper groups (Kohler et al., 2016). We replicate that result using our Bayesian approach, and find an analogous parametric effect in the psychophysical data (see Supplementary Figure 4.1). We also conducted an analysis testing for an effect of index in our two datasets and found that subgroup relationships with higher indices tended to produce greater pairwise differences between the subgroup and supergroup, for both SSVEP RMS and symmetry detection thresholds (see Supplementary Figure 4.2). The effect of index is relatively weak, but the fact that there is a measurable index effect can nonetheless be taken as preliminary evidence that representations of symmetries

174 in wallpaper groups may be compositional.

175 Finally, we conducted a correlation analysis comparing SSVEP and psychophysical data and  
176 found a reliable correlation ( $R^2 = 0.44$ , Bayesian confidence interval [0.28, 0.55]). The correlation  
177 reflects an inverse relationship: For subgroup relationships where the supergroup produces a  
178 much *larger* SSVEP amplitude than the subgroup, the supergroup also tends to produce a much  
179 *smaller* symmetry detection threshold. This is consistent with our hypotheses about how the  
180 two measurements relate to symmetry representations in the brain, and suggests that our brain  
181 imaging and psychophysical measurements are at least to some extent tapping into the same  
182 underlying mechanisms.

## 183 Discussion

184 Here we show that beyond merely responding to the elementary symmetry operations of reflec-  
185 tion (Sasaki et al., 2005; Tyler et al., 2005) and rotation (Kohler et al., 2016), the visual system  
186 represents the hierarchical structure of the 17 wallpaper groups, and thus every combination of  
187 the four fundamental symmetries (rotation, reflection, translation, glide reflection) which com-  
188 prise the set of regular textures. Both SSVEP amplitudes and symmetry detection thresholds  
189 preserve the hierarchy of complexity among the wallpaper groups that is captured by the sub-  
190 group relationships (Coxeter and Moser, 1972). For the SSVEP, this remarkable consistency was  
191 specific to the odd harmonics of the stimulus frequency that are known to capture the symmetry-  
192 specific response (Kohler et al., 2016) and to electrodes in a region-of-interest (ROI) over occipital  
193 cortex. When the same analysis was done using the odd harmonics from electrodes over parietal  
194 cortex (Supplementary Figure 3.3) or even harmonics from electrodes over occipital cortex (Sup-  
195 plementary Figure 3.4), the data was substantially less consistent with the subgroup relationships  
196 (yellow and green lines, Figure 5).

197 The current study uses 16 distinct wallpaper groups, while previous neuroimaging studies  
198 focused on a subset of 4 (Kohler et al., 2016, 2018). This represents a significant conceptual advance,  
199 because it makes it possible to investigate the complete subgroup hierarchy among the 17 groups  
200 and ask to what extent the hierarchy is reflected in brain activity. Our data provide a description  
201 of the visual system's response to the complete set of symmetries in the two-dimensional plane.  
202 We do not independently measure the response to  $P_1$ , but because each of the 16 other groups  
203 produce non-zero odd harmonic amplitudes (see Figure 2), we can conclude that the relationships  
204 between  $P_1$  and all other groups, where  $P_1$  is the subgroup, are also preserved by the visual system.  
205 The subgroup relationships are in many cases not obvious perceptually, and most participants  
206 had no knowledge of group theory. Thus, the visual system's ability to preserve the subgroup  
207 hierarchy does not depend on explicit knowledge of the relationships. Previous brain-imaging  
208 studies have found evidence of parametric responses with the number of reflection symmetry folds  
209 Keefe et al. (2018); Sasaki et al. (2005); Makin et al. (2016) and with the order of rotation symmetry  
210 Kohler et al. (2016). Our study is the first demonstration that the brain encodes symmetry in  
211 this parametric fashion across every possible combination of different *symmetry types*, and that this  
212 parametric encoding is also reflected in behavior. Previous behavioral experiments have shown

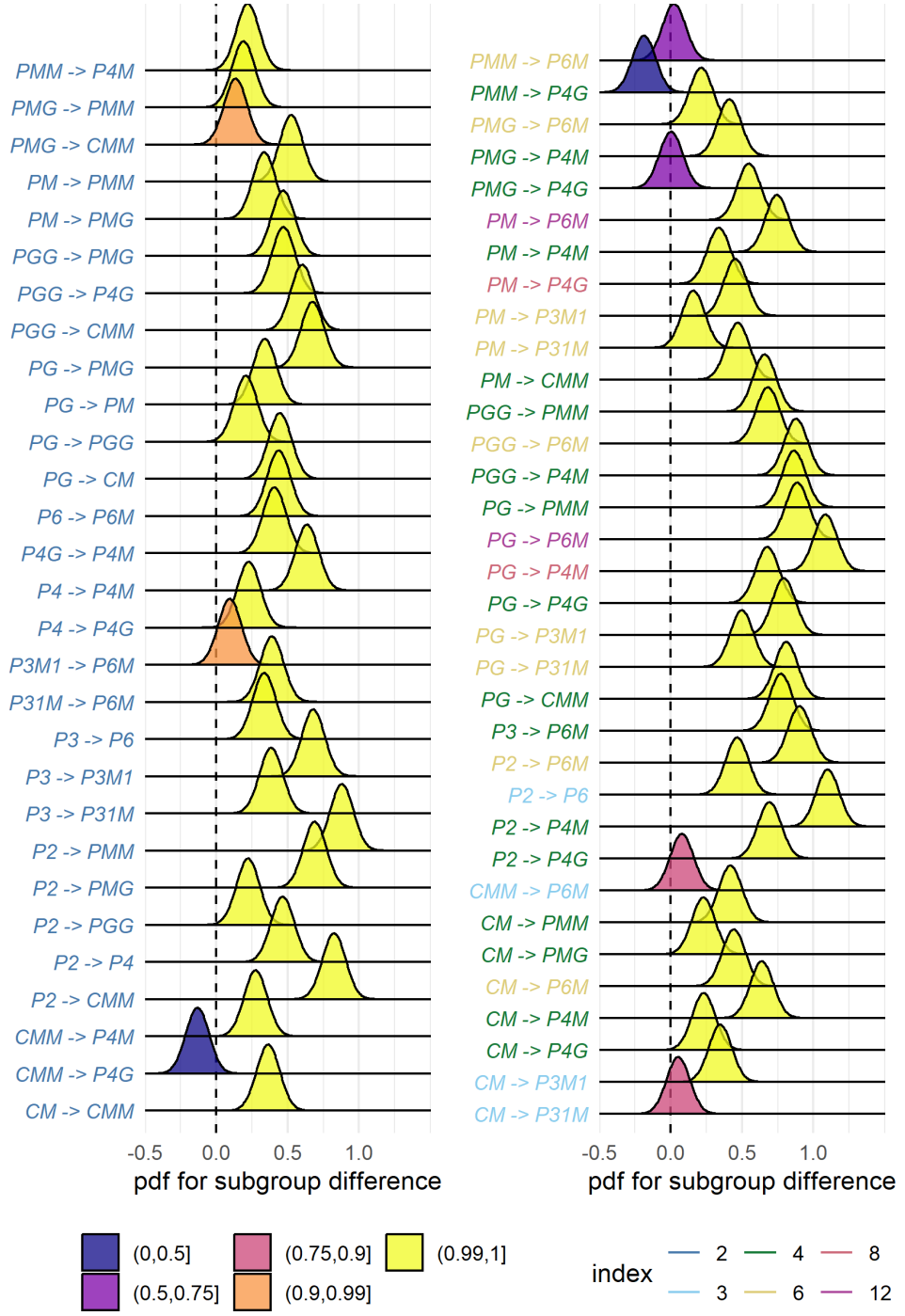


Figure 3: Posterior distributions for the difference in mean SSVEP RMS amplitude. Colour coding of the text indicates the index of the subgroup, while the colour of the filled distribution relates to the conditional probability that the difference in means is greater than zero. We can see that 55/63 subgroup relationships have  $p(\Delta < 0 | \text{data}) > 0.99$ .

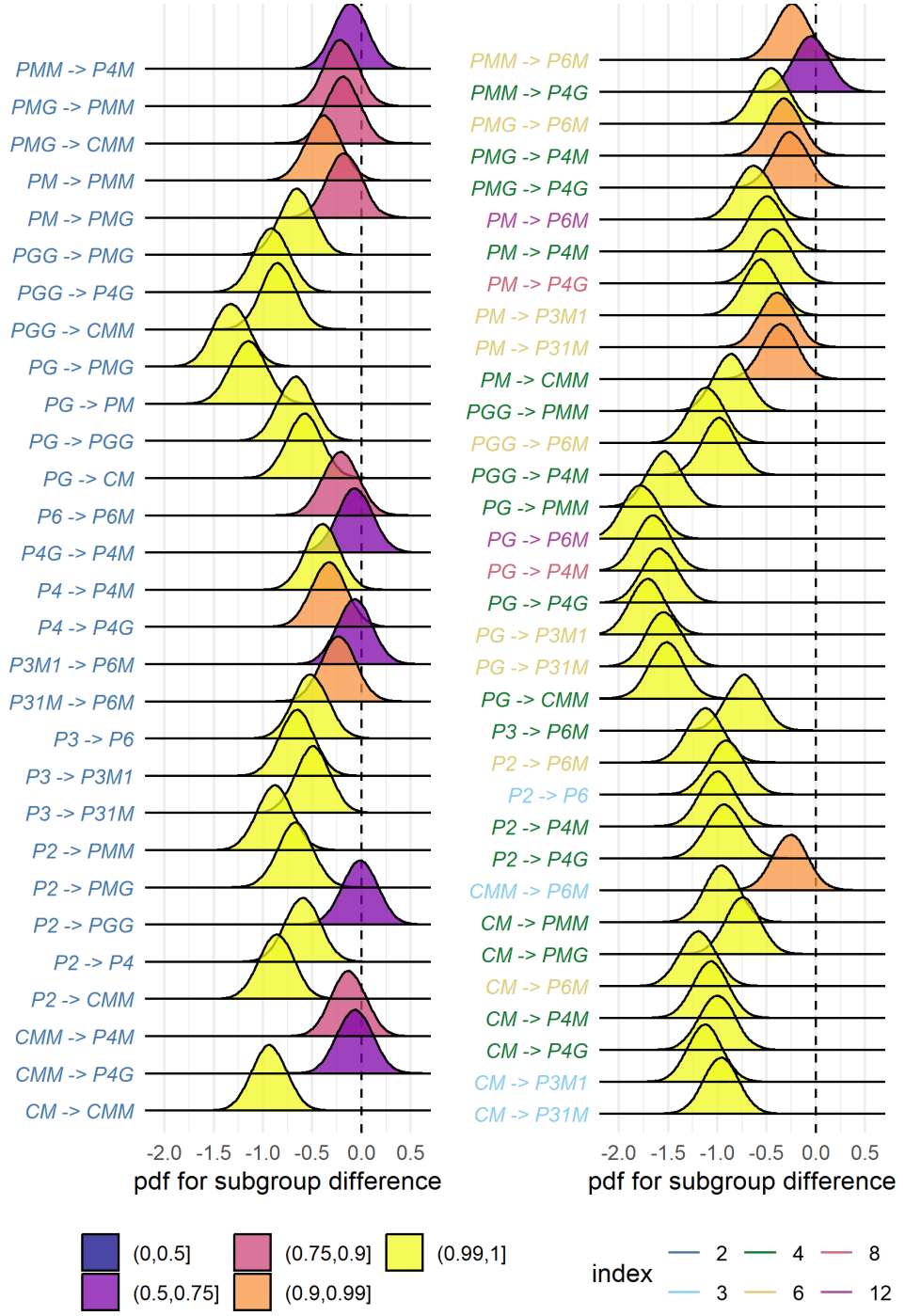


Figure 4: Posterior distributions for the difference in mean symmetry detection threshold durations. Colour coding of the text indicates the index of the subgroup, while the colour of the filled distribution relates to the conditional probability that the difference in means is smaller than zero. We can see that 43/63 subgroup relationships have  $p(\Delta > 0 | \text{data}) > 0.99$ .

that although naïve observers can distinguish many of the wallpaper groups (Landwehr, 2009), they tend to sort exemplars into fewer (4–12) sets than the number of wallpaper groups, often placing exemplars from different wallpaper groups in the same set (Clarke et al., 2011). The two-interval forced choice approach we use in the current psychophysical experiment makes it possible to directly compare symmetry detection thresholds to the subgroup hierarchy, and reveals that not only can the 17 wallpaper groups be distinguished based on behavioral data, behavior largely follows the subgroup hierarchy.

A large literature exists on the *Sustained Posterior Negativity* (SPN), a characteristic negative-going waveform that is known to reflect responses to symmetry and other forms of regularity and structure (Makin et al., 2016). The SPN scales with the proportion of reflection symmetry in displays that contain a mixture of symmetry and noise (Makin et al., 2020; Palumbo et al., 2015), and both reflection, rotation and translation can produce a measurable SPN (Makin et al., 2013). It has recently been demonstrated that a holographic model of regularity (van der Helm and Leeuwenberg, 1996), can predict both SPN amplitude (Makin et al., 2016) and perceptual discrimination performance (Nucci and Wagemans, 2007) for dot patterns that contain symmetry and other types of regularity. The available evidence suggests that the SPN and our SSVEP measurements are two distinct methods for isolating the same symmetry-related brain response: When observed in the time-domain, the symmetry-selective odd-harmonic responses produce similarly sustained waveforms (see Figure 2), odd-harmonic SSVEP responses can be measured for dot patterns similar to those used to measure the SPN (Norcia et al., 2002), and the one event-related study on the wallpaper groups also found SPN-like waveforms (Kohler et al., 2018). Future work should more firmly establish the connection and determine if the SPN can capture similarly precise symmetry responses as the SSVEPs presented here. It would also be worthwhile to ask if and how  $W$  can be computed for our random-noise based wallpaper textures where combinations of symmetries tile the plane.

We observe a reliable correlation between our brain imaging and psychophysical data. This suggests that the two measurements reflect the same underlying symmetry representations in visual cortex. It should be noted that the correlation is relatively modest ( $R^2 = 0.44$ ). This may be partly due to the fact that different individuals participated in the two experiments. It may also be related to the fact that participants were not doing a symmetry-related task during the SSVEP experiment, but instead monitored the stimuli for brief changes in contrast that occurred twice per trial (see Methods). Previous brain imaging studies have found enhanced reflection symmetry responses when participants performed a symmetry-related task (Makin et al., 2020; Sasaki et al., 2005; Keefe et al., 2018). It is possible that adding a symmetry-related task to our SSVEP experiment would have produced measurements that reflected subgroup relationships to an even higher extent than what we observed. On the other hand, our results are already close to ceiling (see Figure 5) and adding a symmetry-related task may simply enhance SSVEP amplitudes overall without improving the discriminability of individual groups, as has been observed for reflection by Keefe et al. (2018). Task-driven processing may be important for detecting symmetries that have been subject to perspective distortion, as suggested by SPN measurements (Makin et al., 2015) and somewhat less clearly in a subsequent functional MRI study (Keefe et al., 2018).

254 Future work in which behavioral and brain imaging data are collected from the same participants,  
255 and task is manipulated in the SSVEP experiment, will help further establish the connection be-  
256 tween the two measurements, and elucidate the potential contribution of task-related top-down  
257 processing to the current results.

258 We also find an effect of index for both our brain imaging measurements and our symmetry  
259 detection thresholds. This means that the visual system not only represents the hierarchical rela-  
260 tionship captured by individual subgroups, but also distinguishes between subgroups depending  
261 on how many times the subgroup is repeated in the supergroup, with more repetitions leading  
262 to larger pairwise differences. Our measured effect of index is relatively weak. This is perhaps  
263 because the index analysis does not take into account the *type* of isometries that differentiate the  
264 subgroup and supergroup. The effect of symmetry type can be observed by contrasting the mea-  
265 sured SSVEP amplitudes and detection thresholds for groups *PM* and *PG* in Figure 2. The two  
266 groups are comparable except *PM* contains reflection and *PG* contains glide reflection, and the  
267 former clearly elicits higher amplitudes and lower thresholds. An important goal for future work  
268 will be to map out how different symmetry types contribute to the representational hierarchy.

269 The correspondence between responses in the visual system and group theory that we demon-  
270 strate here, may reflect a form of implicit learning that depends on the structure of the natural  
271 world. The environment is itself constrained by physical forces underlying pattern formation  
272 and these forces are subject to multiple symmetry constraints (Hoyle, 2006). The ordered struc-  
273 ture of responses to wallpaper groups could be driven by a central tenet of neural coding, that of  
274 efficiency. If coding is to be efficient, neural resources should be distributed to capture the struc-  
275 ture of the environment with minimum redundancy considering the visual geometric optics, the  
276 capabilities of the subsequent neural coding stages and the behavioral goals of the organism (At-  
277 tneave, 1954; Barlow, 1961; Laughlin, 1981; Geisler et al., 2009). Early work within the efficient  
278 coding framework suggested that natural images had a  $1/f$  spectrum and that the corresponding  
279 redundancy between pixels in natural images could be coded efficiently with a sparse set of ori-  
280 ented filter responses, such as those present in the early visual pathway (Field, 1987; Olshausen  
281 and Field, 1997). Our results suggest that the principle of efficient coding extends to a much  
282 higher level of structural redundancy – that of symmetries in visual images.

283 The 17 wallpaper groups are completely regular, and relatively rare in the visual environment,  
284 especially when considering distortions due to perspective (see above) and occlusion. Near-regular  
285 textures, however, abound in the visual world, and can be modeled as deformed versions of the  
286 wallpaper groups (Liu et al., 2004). The correspondence between visual cortex responses and  
287 group theory demonstrated here may indicate that the visual system represents visual textures  
288 using a similar scheme, with the wallpaper groups serving as anchor points in representational  
289 space. This framework resembles norm-based encoding strategies that have been proposed for  
290 other stimulus classes, most notably faces (Leopold et al., 2006), and leads to the prediction that  
291 adaptation to wallpaper patterns should distort perception of near-regular textures, similar to  
292 the aftereffects found for faces (Webster and MacLin, 1999). Field biologists have demonstrated  
293 that animals respond more strongly to exaggerated versions of a learned stimulus, referred to  
294 as “supernormal” stimuli (Tinbergen, 1953). In the norm-based encoding framework, wallpaper

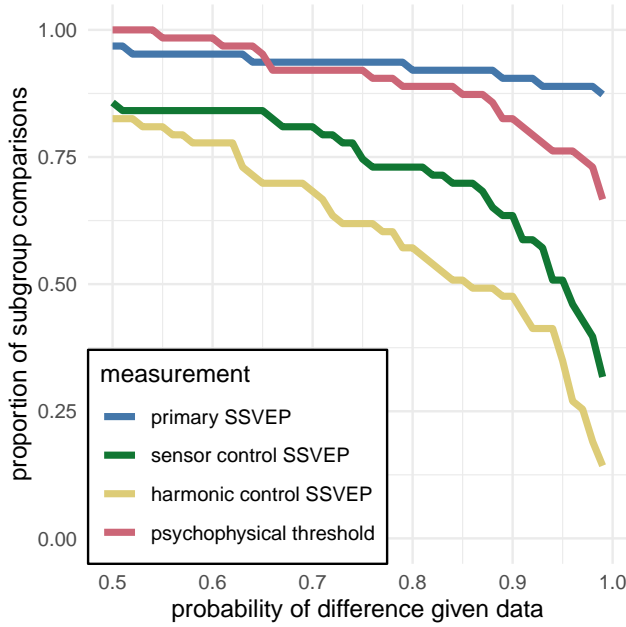


Figure 5: This plot shows the proportion of subgroup relationships that satisfy  $p(\Delta > 0 | \text{data}) > x$  for the SSVEP data and  $p(\Delta < 0 | \text{data}) > x$  for the psychophysical data. We can see that if we take  $x = 0.95$  as our threshold, the subgroup relationships are preserved in  $56/63 = 89\%$  and  $48/63 = 76\%$  of the comparisons for the primary SSVEP and threshold duration datasets, respectively. This compares to the  $32/63 = 51\%$  and  $22/63 = 35\%$  for the SSVEP control datasets.

groups can be considered *supertextures*, exaggerated examples of the near-regular textures common in the natural world. If non-human animals employ a similar encoding strategy, they would be expected to be sensitive to symmetries in wallpaper groups. Recent functional MRI work in macaque monkeys offer some support for that: Macaque visual cortex responds parametrically to reflection and rotation symmetries in wallpaper groups, and the set of brain areas involved largely overlap those observed to be sensitive to symmetry in humans (Audurier et al., 2021). In human societies, visual artists may consciously or unconsciously create supernormal stimuli, to capture the essence of the subject and evoke strong responses in the audience (Ramachandran and Hirstein, 1999). Wallpaper groups are visually compelling, and symmetries have been widely used in human artistic expression going back to the Neolithic age (Jablan, 2014). If wallpapers are in fact supertextures, this prevalence may be a direct result of the strategy the human visual system has adopted for texture encoding.

## Participants

Twenty-five participants (11 females, mean age  $28.7 \pm 3.3$ ) took part in the EEG experiment. Their informed consent was obtained before the experiment under a protocol that was approved by the Institutional Review Board of Stanford University. 11 participants (8 females, mean age  $20.73 \pm 1.21$ ) took part in the psychophysics experiment. All participants had normal or corrected-to-normal vision. Their informed consent was obtained before the experiment under a protocol that was approved by the University of Essex's Ethics Committee. There was no overlap in

314 participants between the EEG and psychophysics experiments.

### 315 Stimulus Generation

316 Exemplars from the different wallpaper groups were generated using a modified version of the  
317 methodology developed by Clarke and colleagues(Clarke et al., 2011) that we have described in de-  
318 tail elsewhere(Kohler et al., 2016). Briefly, exemplar patterns for each group were generated from  
319 random-noise textures, which were then repeated and transformed to cover the plane, according  
320 to the symmetry axes and geometric lattice specific to each group. The use of noise textures as  
321 the starting point for stimulus generation allowed the creation of an almost infinite number of  
322 distinct exemplars of each wallpaper group. To make individual exemplars as similar as possible  
323 we replaced the power spectrum of each exemplar with the median across exemplars within a  
324 group. We then generated control exemplars that had the same power spectrum as the exemplar  
325 images by randomizing the phase of each exemplar image. The phase scrambling eliminates ro-  
326 tation, reflection and glide-reflection symmetries within each exemplar, but the phase-scrambled  
327 images inherit the spectral periodicity arising from the periodic tiling. This means that all  
328 control exemplars, regardless of which wallpaper group they are derived from, are transformed  
329 into another symmetry group, namely  $P_1$ .  $P_1$  is the simplest of the wallpaper groups and contains  
330 only translations of a region whose shape derives from the lattice. Because the different wallpaper  
331 groups have different lattices,  $P_1$  controls matched to different groups have different power spectra.  
332 Our experimental design takes these differences into account by comparing the neural responses  
333 evoked by each wallpaper group to responses evoked by the matched control exemplars.

### 334 Stimulus Presentation

335 Stimulus Presentation. For the EEG experiment, the stimuli were shown on a 24.5" Sony Trimas-  
336 ter EL PVM-2541 organic light emitting diode (OLED) display at a screen resolution of  $1920 \times 1080$   
337 pixels, 8-bit color depth and a refresh rate of 60 Hz, viewed at a distance of 70 cm. The mean  
338 luminance was  $69.93 \text{ cd/m}^2$  and contrast was 95%. The diameter of the circular aperture in  
339 which the wallpaper pattern appeared was  $13.8^\circ$  of visual angle presented against a mean lumi-  
340 nance gray background. Stimulus presentation was controlled using in-house software. For the  
341 psychophysics experiment, the stimuli were shown on a  $48 \times 27\text{cm}$  VIEWPixx/3D LCD Display  
342 monitor, model VPX-VPX-2005C, resolution  $1920 \times 1080$  pixels, with a viewing distance of ap-  
343 proximately 40cm and linear gamma. Stimulus presentation was controlled using MatLab and  
344 Psychtoolbox-3 (Kleiner et al., 2007; Brainard, 1997). The diameter of the circular aperture for  
345 the stimuli was  $21.5^\circ$ .

### 346 EEG Procedure

347 Visual Evoked Potentials were measured using a steady-state design, in which  $P_1$  control images  
348 alternated with exemplar images from each of the 16 other wallpaper groups. Exemplar images  
349 were always preceded by their matched  $P_1$  control image. A single 0.83 Hz stimulus cycle consisted  
350 of a control  $P_1$  image followed by an exemplar image, each shown for 600 ms. A trial consisted of 10

such cycles (12 sec) over which 10 different exemplar images and matched controls from the same rotation group were presented. For each group type, the individual exemplar images were always shown in the same order within the trials. Participants initiated each trial with a button-press, which allowed them to take breaks between trials. Trials from a single wallpaper group were presented in blocks of four repetitions, which were themselves repeated twice per session, and shown in random order within each session. To control fixation, the participants were instructed to fixate a small white cross in the center of display. To control vigilance, a contrast dimming task was employed. Two times per trial, an image pair (control  $P_1$  plus exemplar) was shown at reduced contrast. Participants were instructed to press a button on a response pad whenever they noticed a contrast change. Reaction times were not taken into account and participants were told to respond at their own pace while being as accurate as possible. We adjusted the reduction in contrast such that average accuracy for each participant was kept at 85% correct, in order to keep the difficulty of the vigilance task at a constant level.

## Psychophysics Procedure

The experiment consisted of 16 blocks, one for each of the wallpaper groups (excluding  $P_1$ ). We used a two-interval forced choice approach. In each trial, participants were presented with two stimuli (one of which was the wallpaper group for the current block of trials, the other being  $P_1$ ), one after the other (inter-stimulus interval of 700ms). After each stimulus had been presented, it was masked with white noise for 300ms. After both stimuli had been presented, participants made a response on the keyboard to indicate whether they thought the first or second image contained more symmetry. Each block started with 10 practice trials, (stimulus display duration of 500ms) to allow participants to familiarise themselves with the current block's wallpaper pattern. If they achieved an accuracy of 9/10 in these trials they progressed to the rest of the block, otherwise they carried out another set of 10 practise trials. This process was repeated until the required accuracy of 9/10 was obtained. The rest of the block consisted of four interleaved staircases (using the QUEST algorithm (Watson and Pelli, 1983), full details given in the SI) of 30 trials each. On average, a block of trials took around 10 minutes to complete.

## EEG Acquisition and Preprocessing

Steady-State Visual Evoked Potentials (SSVEPs) were collected with 128-sensor HydroCell Sensor Nets (Electrical Geodesics, Eugene, OR) and were band-pass filtered from 0.3 to 50 Hz. Raw data were evaluated off line according to a sample-by-sample thresholding procedure to remove noisy sensors that were replaced by the average of the six nearest spatial neighbors. On average, less than 5% of the electrodes were substituted; these electrodes were mainly located near the forehead or the ears. The substitutions can be expected to have a negligible impact on our results, as the majority of our signal can be expected to come from electrodes over occipital, temporal and parietal cortices. After this operation, the waveforms were re-referenced to the common average of all the sensors. The data from each 12s trial were segmented into five 2.4 s long epochs (i.e., each of these epochs was exactly 2 cycles of image modulation). Epochs for which a large percentage of data samples exceeding a noise threshold (depending on the participant and ranging between 25

and  $50 \mu\text{V}$ ) were excluded from the analysis on a sensor-by-sensor basis. This was typically the case for epochs containing artifacts, such as blinks or eye movements. Steady-state stimulation will drive cortical responses at specific frequencies directly tied to the stimulus frequency. It is thus appropriate to quantify these responses in terms of both phase and amplitude. Therefore, a Fourier analysis was applied on every remaining epoch using a discrete Fourier transform with a rectangular window. The use of two-cycle long epochs (i.e., 2.4 s) was motivated by the need to have a relatively high resolution in the frequency domain,  $\delta f = 0.42 \text{ Hz}$ . For each frequency bin, the complex-valued Fourier coefficients were then averaged across all epochs within each trial. Each participant did two sessions of 8 trials per condition, which resulted in a total of 16 trials per condition.

## SSVEP Analysis

Response waveforms were generated for each group by selective filtering in the frequency domain. For each participant, the average Fourier coefficients from the two sessions were averaged over trials and sessions. The SSVEP paradigm we used allowed us to separate symmetry-related responses from non-specific contrast transient responses. Previous work has demonstrated that symmetry-related responses are predominantly found in the odd harmonics of the stimulus frequency, whereas the even harmonics consist mainly of responses unrelated to symmetry, that arise from the contrast change associated with the appearance of the second image (Norcia et al., 2002; Kohler et al., 2016). This functional distinction of the harmonics allowed us to generate a single-cycle waveform containing the response specific to symmetry, by filtering out the even harmonics in the spectral domain, and then back-transforming the remaining signal, consisting only of odd harmonics, into the time-domain. For our main analysis, we averaged the odd harmonic single-cycle waveforms within a six-electrode region of interest (ROI) over occipital cortex (electrodes 70, 74, 75, 81, 82, 83). These waveforms, averaged over participants, are shown in Figure 2. The same analysis was done for the even harmonics and for the odd harmonics within a six electrode ROI over parietal cortex (electrodes 53, 54, 61, 78, 79, 86; see Supplementary Figure 1.1). The root-mean square values of these waveforms, for each individual participant, were used to determine whether each of the wallpaper subgroup relationships were preserved in the brain data.

## Defining the list of subgroup relationships

In order to get the complete list of subgroup relationships, we digitized Table 4 from Coxeter (Coxeter and Moser, 1972) (shown in Supplementary Table 1.2). After removing identity relationships (i.e. each group is a subgroup of itself) and the three pairs of wallpaper groups that are subgroups of each other (e.g. *PM* is a subgroup of *CM*, and *CM* is a subgroup of *PM*) we were left with a total of 63 unambiguous subgroups that were included in our analysis.

## 425 Bayesian Analysis of SSVEP and Psychophysical data

426 Bayesian analysis was carried out using R (v3.6.1) (R Core Team, 2019) with the `brms` package  
427 (v2.9.0) (Bürkner, 2017) and rStan (v2.19.2 (Stan Development Team, 2019)). The data from each  
428 experiment were modelled using a Bayesian generalised mixed effect model with wallpaper group  
429 being treated as a 16-level factor, and random effects for participant. The SSVEP data and sym-  
430 metry detection threshold durations were modelled using log-normal distributions with weakly  
431 informative,  $\mathcal{N}(0, 2)$ , priors. After fitting the model to the data, samples were drawn from the  
432 posterior distribution of the two datasets, for each wallpaper group. These samples were then  
433 recombined to calculate the distribution of differences for each of the 63 pairs of subgroup and  
434 supergroup. These distributions were then summarised by computing the conditional probabil-  
435 ity of obtaining a positive (negative) difference,  $p(\Delta|\text{data})$ . For further technical details, please  
436 see the Supplementary Materials where the full R code, model specification, prior and posterior  
437 predictive checks, and model diagnostics, can be found.

## 438 Acknowledgments

439 The authors would like to thank two anonymous reviewers whose comments helped improve and  
440 clarify the manuscript, and also express their gratitude to Professor Anthony M. Norcia for his  
441 invaluable mentorship and contribution to our thinking about the role of symmetry in vision,  
442 and about vision and the brain more generally, through years of collaboration and discussions.

443 This work was supported by the Vision Science to Applications (VISTA) program funded by the  
444 Canada First Research Excellence Fund (CFREF, 2016–2023) and by a Discovery Grant from the  
445 Natural Sciences and Engineering Research Council of Canada awarded to PJK. The work was  
446 also partially supported by a National Science Foundation INSPIRE grant 1248076 awarded to  
447 Yanxi Liu, Anthony M. Norcia and Rick O. Gilmore. A preliminary version of the EEG portion  
448 of the manuscript was previously deposited on bioRxiv.

## 449 Data Accessibility

450 Data from the EEG and Psychophysics experiments have been made available with the Supple-  
451 mentary Material on OSF.

## 452 References

- 453 Apthorp, D. and Bell, J. (2015). Symmetry is less than  
454 meets the eye. *Current Biology*, 25(7):R267–R268.  
455 Attneave, F. (1954). Some informational aspects of  
456 visual perception. *Psychol Rev*, 61(3):183–93.  
457 Audurier, P., Héjja-Brichard, Y., Castro, V. D.,  
458 Kohler, P. J., Norcia, A. M., Durand, J.-B., and  
459 Cottereau, B. R. (2021). Symmetry processing  
460 in the macaque visual cortex. *bioRxiv*, page  
461 2021.03.13.435181. Publisher: Cold Spring Harbor  
462 Laboratory Section: New Results.  
463 Barlow, H. B. (1961). *Possible principles underlying the  
464 transformations of sensory messages*, pages 217–234.  
465 MIT Press.  
466 Brainard, D. H. (1997). Spatial vision. *The psy-  
467 chophysics toolbox*, 10:433–436.  
468 Bürkner, P.-C. (2017). Advanced bayesian multilevel  
469 modeling with the r package brms. *arXiv preprint  
470 arXiv:1705.11123*.

- 471 Clarke, A. D. F., Green, P. R., Halley, F., and  
 472 Chantler, M. J. (2011). Similar symmetries: The  
 473 role of wallpaper groups in perceptual texture simi-  
 474 larity. *Symmetry*, 3(4):246–264.
- 475 Cohen, E. H. and Zaidi, Q. (2013). Symmetry in con-  
 476 text: Salience of mirror symmetry in natural pat-  
 477 terns. *Journal of vision*, 13(6).
- 478 Coxeter, H. S. M. and Moser, W. O. J. (1972). *Gener-  
 479 ators and relations for discrete groups*. Ergebnisse  
 480 der Mathematik und ihrer Grenzgebiete ; Bd. 15.  
 481 Springer-Verlag, Berlin, New York.
- 482 Fedorov, E. (1891). Symmetry in the plane. In *Za-  
 483 piski Imperatorskogo S. Peterburgskogo Mineralogicheskogo  
 484 Obshchestva [Proc. S. Peterb. Mineral. Soc.]*, volume 2,  
 485 pages 345–390.
- 486 Field, D. J. (1987). Relations between the statistics  
 487 of natural images and the response properties of  
 488 cortical cells. *J Opt Soc Am A*, 4(12):2379–94.
- 489 Geisler, W. S., Najemnik, J., and Ing, A. D. (2009). Opti-  
 490 mal stimulus encoders for natural tasks. *Journal of Vision*, 9(13):17–17.
- 492 Giurfa, M., Eichmann, B., and Menzel, R. (1996).  
 493 Symmetry perception in an insect. *Nature*,  
 494 382(6590):458–461. Number: 6590 Publisher: Na-  
 495 ture Publishing Group.
- 496 Hamada, J. and Ishihara, T. (1988). Complexity and  
 497 goodness of dot patterns varying in symmetry. *Psy-  
 498 chological Research*, 50(3):155–161.
- 499 Hoyle, R. B. (2006). *Pattern formation: an introduction  
 500 to methods*. Cambridge University Press.
- 501 Jablan, S. V. (2014). *Symmetry, Ornament and Modular-  
 502 ity*. World Scientific Publishing Co Pte Ltd, Singa-  
 503 pore, SINGAPORE.
- 504 Keefe, B. D., Gouws, A. D., Sheldon, A. A., Vernon,  
 505 R. J. W., Lawrence, S. J. D., McKeefry, D. J., Wade,  
 506 A. R., and Morland, A. B. (2018). Emergence of  
 507 symmetry selectivity in the visual areas of the  
 508 human brain: fMRI responses to symmetry pre-  
 509 sented in both frontoparallel and slanted planes.  
*Human Brain Mapping*, 39(10):3813–3826.
- 514 Kleiner, M., Brainard, D., Pelli, D., Ingling, A., Mur-  
 515 ray, R., and Broussard, C. (2007). What's new in  
 psychtoolbox-3. *Perception*, 36:1–16.
- 517 Kohler, P. J., Clarke, A., Yakovleva, A., Liu, Y., and  
 518 Norcia, A. M. (2016). Representation of maximally  
 519 regular textures in human visual cortex. *The Jour-  
 520 nal of Neuroscience*, 36(3):714–729.
- 521 Kohler, P. J., Cottreau, B. R., and Norcia, A. M.  
 522 (2018). Dynamics of perceptual decisions about  
 523 symmetry in visual cortex. *NeuroImage*, 167(Sup-  
 524 pliment C):316–330.
- 525 Landwehr, K. (2009). Camouflaged symmetry. *Per-  
 526 ception*, 38:1712–1720.
- 528 Laughlin, S. (1981). A simple coding procedure en-  
 529 hances a neuron's information capacity. *Z Natur-  
 530 forsch C*, 36(9-10):910–2.
- 531 Leopold, D. A., Bondar, I. V., and Giese, M. A.  
 532 (2006). Norm-based face encoding by single neu-  
 533 rons in the monkey inferotemporal cortex. *Nature*,  
 442(7102):572–5.
- 535 Li, Y., Sawada, T., Shi, Y., Steinman, R., and Pizlo, Z.  
 536 (2013). *Symmetry Is the sine qua non of Shape*, book sec-  
 537 tion 2, pages 21–40. Advances in Computer Vision  
 538 and Pattern Recognition. Springer London.
- 539 Liu, Y., Hel-Or, H., Kaplan, C. S., and Van Gool,  
 540 L. (2010). Computational symmetry in computer  
 541 vision and computer graphics. *Foundations and  
 Trends® in Computer Graphics and Vision*, 5(1–2):1–  
 195.
- 544 Liu, Y., Lin, W.-C., and Hays, J. (2004). Near-regular  
 545 texture analysis and manipulation. In *ACM Trans-  
 546 actions on Graphics (TOG)*, volume 23, pages 368–  
 547 376. ACM.
- 548 Mach, E. (1959). *The Analysis of Sensations* (1897).  
 549 English transl., Dover, New York.
- 550 Makin, A. D. J., Ramponi, G., and Bertamini, M.  
 551 (2015). Conditions for view invariance in  
 552 the neural response to visual symmetry. *Psychophysiology*, 52(4):532–543. eprint:  
<https://onlinelibrary.wiley.com/doi/pdf/10.1111/psyp.12365>

- 551 Makin, A. D. J., Rampone, G., Morris, A., and  
 552 Bertamini, M. (2020). The Formation of Symmetric  
 553 cal Gestalts Is Task-Independent, but Can Be En-  
 554 hanced by Active Regularity Discrimination. *Jour-  
 555 nal of Cognitive Neuroscience*, 32(2):353–366.  
 596
- 556 Makin, A. D. J., Rampone, G., Pecchinenda,  
 557 A., and Bertamini, M. (2013). Electrophysiological  
 558 responses to visuospatial regularity.  
 559 *Psychophysiology*, 50(10):1045–1055. eprint:  
 560 https://onlinelibrary.wiley.com/doi/pdf/10.1111/psyp.12082.  
 601
- 561 Makin, A. D. J., Rampone, G., Wright, A., Marti-  
 562 novic, J., and Bertamini, M. (2014). Visual symme-  
 563 try in objects and gaps. *Journal of Vision*, 14(3):12–  
 564 12. Publisher: The Association for Research  
 565 Vision and Ophthalmology.  
 605
- 566 Makin, A. D. J., Wilton, M. M., Pecchinenda, A., and  
 567 Bertamini, M. (2012). Symmetry perception and af-  
 568 fective responses: A combined EEG/EMG study.  
 569 *Neuropsychologia*, 50(14):3250–3261.  
 610
- 570 Makin, A. D. J., Wright, D., Rampone, G., Palumbo,  
 571 L., Guest, M., Sheehan, R., Cleaver, H., and  
 572 Bertamini, M. (2016). An Electrophysiological  
 573 Index of Perceptual Goodness. *Cerebral Cortex*,  
 574 26(12):4416–4434.  
 615
- 575 Morris, M. R. and Casey, K. (1998). Female sword-  
 576 tail fish prefer symmetrical sexual signal. *Animal*  
 577 *Behaviour*, 55(1):33–39.  
 618
- 578 Møller, A. P. (1992). Female swallow preference  
 579 for symmetrical male sexual ornaments. *Nature*,  
 580 357(6375):238–240.  
 621
- 581 Norcia, A. M., Appelbaum, L. G., Ales, J. M., Col-  
 582 tereau, B. R., and Rossion, B. (2015). The steady-  
 583 state visual evoked potential in vision research: A  
 584 review. *Journal of Vision*, 15(6):4–4.  
 625
- 585 Norcia, A. M., Candy, T. R., Pettet, M. W., Vildavski,  
 586 V. Y., and Tyler, C. W. (2002). Temporal dynam-  
 587 ics of the human response to symmetry. *Journal of  
 588 Vision*, 2(2):132–139.  
 629
- 589 Nucci, M. and Wagemans, J. (2007). Goodness of  
 590 Regularity in Dot Patterns: Global Symmetry, Lo-  
 591 cal Symmetry, and Their Interactions. *Perception*,  
 596 36(9):1305–1319. Publisher: SAGE Publications  
 Ltd STM.
- Ogden, R., Makin, A. D. J., Palumbo, L., and  
 Bertamini, M. (2016). Symmetry Lasts Longer  
 Than Random, but Only for Brief Presentations.  
*i-Perception*, 7(6):2041669516676824. Publisher:  
 SAGE Publications.
- Olshausen, B. A. and Field, D. J. (1997). Sparse cod-  
 ing with an overcomplete basis set: a strategy em-  
 ployed by v1? *Vision Res*, 37(23):3311–25.
- Palmer, S. E. (1985). The role of symmetry in shape  
 perception. *Acta Psychologica*, 59(1):67–90.
- Palmer, S. E. (1991). Goodness, Gestalt, groups, and  
 Garner: Local symmetry subgroups as a theory  
 of figural goodness. In *The perception of structure: Essays in honor of Wendell R. Garner*, pages 23–39. American Psychological Association, Washington, DC, US.
- Palumbo, L., Bertamini, M., and Makin, A. (2015). Scaling of the extrastriate neural response to symmetry. *Vision Research*, 117:1–8.
- Polya, G. (1924). Xii. Über die analogie der kristallsymmetrie in der ebene. *Zeitschrift für Kristallographie-Crystalline Materials*, 60(1):278–282.
- R Core Team (2019). *R: A Language and Environment for Statistical Computing*. R Foundation for Statistical Computing, Vienna, Austria.
- Ramachandran, V. S. and Hirstein, W. (1999). The science of art: A neurological theory of aesthetic experience. *Journal of Consciousness Studies*, 6(6–7):15–41.
- Rhodes, G., Proffitt, F., Grady, J. M., and Sumich, A. (1998). Facial symmetry and the perception of beauty. *Psychonomic Bulletin & Review*, 5(4):659–669.
- Royer, F. L. (1981). Detection of symmetry. *Journal of Experimental Psychology: Human Perception and Performance*, 7(6):1186–1210.
- Sasaki, Y., Vanduffel, W., Knutson, T., Tyler, C., and Tootell, R. (2005). Symmetry activates extrastriate visual cortex in human and nonhuman primates.

- 633     *Proceedings of the National Academy of Sciences of the*  
 634     *United States of America*, 102(8):3159–3163. 660  
 635     Schlüter, A., Parzefall, J., and Schlupp, I. (1998). 661  
 636     male preference for symmetrical vertical bars in 662  
 637     male sailfin mollies. *Animal Behaviour*, 56(1):147–663  
 638     153. 664  
 639     Stan Development Team (2019). RStan: the R inter- 665  
 640     face to Stan. R package version 2.19.2. 666  
 641     Swaddle, J. P. (1999). Visual signalling by asymme- 667  
 642     try: a review of perceptual processes. *Philosophical 668  
 643     Transactions of the Royal Society of London. Series B: 669  
 644     Biological Sciences*. Publisher: The Royal Society. 670  
 645     Swaddle, J. P. and Cuthill, I. C. (1994). Preference for 671  
 646     symmetric males by female zebra finches. *Nature*, 367(6459):165–166. Number: 6459 Publisher: Na- 672  
 647     ture Publishing Group. 673  
 648     Tinbergen, N. (1953). *The herring gull's world: a study 674  
 649     of the social behaviour of birds*. Frederick A. Praeger,  
 650     Inc., Oxford, England. 675  
 651  
 652     Tyler, C. W., Baseler, H. A., Kontsevich, L. 676  
 653     Likova, L. T., Wade, A. R., and Wandell, B. 677  
 654     (2005). Predominantly extra-retinotopic corti- 678  
 655     cal response to pattern symmetry. *Neuroimage*, 24(2):306–314. 679  
 656  
 657     van der Helm, P. A. and Leeuwenberg, E. L. J. (1996).  
 658     Goodness of visual regularities: A nontransfor- 680  
 659     mational approach. *Psychological Review*, 103(3):420–681  
 660  
 661  
 662  
 663  
 664  
 665  
 666  
 667  
 668  
 669  
 670  
 671  
 672  
 673  
 674  
 675  
 676  
 677  
 678  
 679  
 680  
 681  
 682  
 683  
 684  
 685  
 686  
 687  
 688  
 689  
 690  
 691  
 692  
 693  
 694  
 695  
 696  
 697  
 698  
 699  
 700  
 701  
 702  
 703  
 704  
 705  
 706  
 707  
 708  
 709  
 710  
 711  
 712  
 713  
 714  
 715  
 716  
 717  
 718  
 719  
 720  
 721  
 722  
 723  
 724  
 725  
 726  
 727  
 728  
 729  
 730  
 731  
 732  
 733  
 734  
 735  
 736  
 737  
 738  
 739  
 740  
 741  
 742  
 743  
 744  
 745  
 746  
 747  
 748  
 749  
 750  
 751  
 752  
 753  
 754  
 755  
 756  
 757  
 758  
 759  
 760  
 761  
 762  
 763  
 764  
 765  
 766  
 767  
 768  
 769  
 770  
 771  
 772  
 773  
 774  
 775  
 776  
 777  
 778  
 779  
 780  
 781  
 782  
 783  
 784  
 785  
 786  
 787  
 788  
 789  
 790  
 791  
 792  
 793  
 794  
 795  
 796  
 797  
 798  
 799  
 800  
 801  
 802  
 803  
 804  
 805  
 806  
 807  
 808  
 809  
 810  
 811  
 812  
 813  
 814  
 815  
 816  
 817  
 818  
 819  
 820  
 821  
 822  
 823  
 824  
 825  
 826  
 827  
 828  
 829  
 830  
 831  
 832  
 833  
 834  
 835  
 836  
 837  
 838  
 839  
 840  
 841  
 842  
 843  
 844  
 845  
 846  
 847  
 848  
 849  
 850  
 851  
 852  
 853  
 854  
 855  
 856  
 857  
 858  
 859  
 860  
 861  
 862  
 863  
 864  
 865  
 866  
 867  
 868  
 869  
 870  
 871  
 872  
 873  
 874  
 875  
 876  
 877  
 878  
 879  
 880  
 881  
 882  
 883  
 884  
 885  
 886  
 887  
 888  
 889  
 890  
 891  
 892  
 893  
 894  
 895  
 896  
 897  
 898  
 899  
 900  
 901  
 902  
 903  
 904  
 905  
 906  
 907  
 908  
 909  
 910  
 911  
 912  
 913  
 914  
 915  
 916  
 917  
 918  
 919  
 920  
 921  
 922  
 923  
 924  
 925  
 926  
 927  
 928  
 929  
 930  
 931  
 932  
 933  
 934  
 935  
 936  
 937  
 938  
 939  
 940  
 941  
 942  
 943  
 944  
 945  
 946  
 947  
 948  
 949  
 950  
 951  
 952  
 953  
 954  
 955  
 956  
 957  
 958  
 959  
 960  
 961  
 962  
 963  
 964  
 965  
 966  
 967  
 968  
 969  
 970  
 971  
 972  
 973  
 974  
 975  
 976  
 977  
 978  
 979  
 980  
 981  
 982  
 983  
 984  
 985  
 986  
 987  
 988  
 989  
 990  
 991  
 992  
 993  
 994  
 995  
 996  
 997  
 998  
 999  
 1000  
 1001  
 1002  
 1003  
 1004  
 1005  
 1006  
 1007  
 1008  
 1009  
 1010  
 1011  
 1012  
 1013  
 1014  
 1015  
 1016  
 1017  
 1018  
 1019  
 1020  
 1021  
 1022  
 1023  
 1024  
 1025  
 1026  
 1027  
 1028  
 1029  
 1030  
 1031  
 1032  
 1033  
 1034  
 1035  
 1036  
 1037  
 1038  
 1039  
 1040  
 1041  
 1042  
 1043  
 1044  
 1045  
 1046  
 1047  
 1048  
 1049  
 1050  
 1051  
 1052  
 1053  
 1054  
 1055  
 1056  
 1057  
 1058  
 1059  
 1060  
 1061  
 1062  
 1063  
 1064  
 1065  
 1066  
 1067  
 1068  
 1069  
 1070  
 1071  
 1072  
 1073  
 1074  
 1075  
 1076  
 1077  
 1078  
 1079  
 1080  
 1081  
 1082  
 1083  
 1084  
 1085  
 1086  
 1087  
 1088  
 1089  
 1090  
 1091  
 1092  
 1093  
 1094  
 1095  
 1096  
 1097  
 1098  
 1099  
 1100  
 1101  
 1102  
 1103  
 1104  
 1105  
 1106  
 1107  
 1108  
 1109  
 1110  
 1111  
 1112  
 1113  
 1114  
 1115  
 1116  
 1117  
 1118  
 1119  
 1120  
 1121  
 1122  
 1123  
 1124  
 1125  
 1126  
 1127  
 1128  
 1129  
 1130  
 1131  
 1132  
 1133  
 1134  
 1135  
 1136  
 1137  
 1138  
 1139  
 1140  
 1141  
 1142  
 1143  
 1144  
 1145  
 1146  
 1147  
 1148  
 1149  
 1150  
 1151  
 1152  
 1153  
 1154  
 1155  
 1156  
 1157  
 1158  
 1159  
 1160  
 1161  
 1162  
 1163  
 1164  
 1165  
 1166  
 1167  
 1168  
 1169  
 1170  
 1171  
 1172  
 1173  
 1174  
 1175  
 1176  
 1177  
 1178  
 1179  
 1180  
 1181  
 1182  
 1183  
 1184  
 1185  
 1186  
 1187  
 1188  
 1189  
 1190  
 1191  
 1192  
 1193  
 1194  
 1195  
 1196  
 1197  
 1198  
 1199  
 1200  
 1201  
 1202  
 1203  
 1204  
 1205  
 1206  
 1207  
 1208  
 1209  
 1210  
 1211  
 1212  
 1213  
 1214  
 1215  
 1216  
 1217  
 1218  
 1219  
 1220  
 1221  
 1222  
 1223  
 1224  
 1225  
 1226  
 1227  
 1228  
 1229  
 1230  
 1231  
 1232  
 1233  
 1234  
 1235  
 1236  
 1237  
 1238  
 1239  
 1240  
 1241  
 1242  
 1243  
 1244  
 1245  
 1246  
 1247  
 1248  
 1249  
 1250  
 1251  
 1252  
 1253  
 1254  
 1255  
 1256  
 1257  
 1258  
 1259  
 1260  
 1261  
 1262  
 1263  
 1264  
 1265  
 1266  
 1267  
 1268  
 1269  
 1270  
 1271  
 1272  
 1273  
 1274  
 1275  
 1276  
 1277  
 1278  
 1279  
 1280  
 1281  
 1282  
 1283  
 1284  
 1285  
 1286  
 1287  
 1288  
 1289  
 1290  
 1291  
 1292  
 1293  
 1294  
 1295  
 1296  
 1297  
 1298  
 1299  
 1300  
 1301  
 1302  
 1303  
 1304  
 1305  
 1306  
 1307  
 1308  
 1309  
 1310  
 1311  
 1312  
 1313  
 1314  
 1315  
 1316  
 1317  
 1318  
 1319  
 1320  
 1321  
 1322  
 1323  
 1324  
 1325  
 1326  
 1327  
 1328  
 1329  
 1330  
 1331  
 1332  
 1333  
 1334  
 1335  
 1336  
 1337  
 1338  
 1339  
 1340  
 1341  
 1342  
 1343  
 1344  
 1345  
 1346  
 1347  
 1348  
 1349  
 1350  
 1351  
 1352  
 1353  
 1354  
 1355  
 1356  
 1357  
 1358  
 1359  
 1360  
 1361  
 1362  
 1363  
 1364  
 1365  
 1366  
 1367  
 1368  
 1369  
 1370  
 1371  
 1372  
 1373  
 1374  
 1375  
 1376  
 1377  
 1378  
 1379  
 1380  
 1381  
 1382  
 1383  
 1384  
 1385  
 1386  
 1387  
 1388  
 1389  
 1390  
 1391  
 1392  
 1393  
 1394  
 1395  
 1396  
 1397  
 1398  
 1399  
 1400  
 1401  
 1402  
 1403  
 1404  
 1405  
 1406  
 1407  
 1408  
 1409  
 1410  
 1411  
 1412  
 1413  
 1414  
 1415  
 1416  
 1417  
 1418  
 1419  
 1420  
 1421  
 1422  
 1423  
 1424  
 1425  
 1426  
 1427  
 1428  
 1429  
 1430  
 1431  
 1432  
 1433  
 1434  
 1435  
 1436  
 1437  
 1438  
 1439  
 1440  
 1441  
 1442  
 1443  
 1444  
 1445  
 1446  
 1447  
 1448  
 1449  
 1450  
 1451  
 1452  
 1453  
 1454  
 1455  
 1456  
 1457  
 1458  
 1459  
 1460  
 1461  
 1462  
 1463  
 1464  
 1465  
 1466  
 1467  
 1468  
 1469  
 1470  
 1471  
 1472  
 1473  
 1474  
 1475  
 1476  
 1477  
 1478  
 1479  
 1480  
 1481  
 1482  
 1483  
 1484  
 1485  
 1486  
 1487  
 1488  
 1489  
 1490  
 1491  
 1492  
 1493  
 1494  
 1495  
 1496  
 1497  
 1498  
 1499  
 1500  
 1501  
 1502  
 1503  
 1504  
 1505  
 1506  
 1507  
 1508  
 1509  
 1510  
 1511  
 1512  
 1513  
 1514  
 1515  
 1516  
 1517  
 1518  
 1519  
 1520  
 1521  
 1522  
 1523  
 1524  
 1525  
 1526  
 1527  
 1528  
 1529  
 1530  
 1531  
 1532  
 1533  
 1534  
 1535  
 1536  
 1537  
 1538  
 1539  
 1540  
 1541  
 1542  
 1543  
 1544  
 1545  
 1546  
 1547  
 1548  
 1549  
 1550  
 1551  
 1552  
 1553  
 1554  
 1555  
 1556  
 1557  
 1558  
 1559  
 1560  
 1561  
 1562  
 1563  
 1564  
 1565  
 1566  
 1567  
 1568  
 1569  
 1570  
 1571  
 1572  
 1573  
 1574  
 1575  
 1576  
 1577  
 1578  
 1579  
 1580  
 1581  
 1582  
 1583  
 1584  
 1585  
 1586  
 1587  
 1588  
 1589  
 1590  
 1591  
 1592  
 1593  
 1594  
 1595  
 1596  
 1597  
 1598  
 1599  
 1600  
 1601  
 1602  
 1603  
 1604  
 1605  
 1606  
 1607  
 1608  
 1609  
 1610  
 1611  
 1612  
 1613  
 1614  
 1615  
 1616  
 1617  
 1618  
 1619  
 1620  
 1621  
 1622  
 1623  
 1624  
 1625  
 1626  
 1627  
 1628  
 1629  
 1630  
 1631  
 1632  
 1633  
 1634  
 1635  
 1636  
 1637  
 1638  
 1639  
 1640  
 1641  
 1642  
 1643  
 1644  
 1645  
 1646  
 1647  
 1648  
 1649  
 1650  
 1651  
 1652  
 1653  
 1654  
 1655  
 1656  
 1657  
 1658  
 1659  
 1660  
 1661  
 1662  
 1663  
 1664  
 1665  
 1666  
 1667  
 1668  
 1669  
 1670  
 1671  
 1672  
 1673  
 1674  
 1675  
 1676  
 1677  
 1678  
 1679  
 1680  
 1681  
 1682  
 1683  
 1684  
 1685  
 1686  
 1687  
 1688  
 1689  
 1690  
 1691  
 1692  
 1693  
 1694  
 1695  
 1696  
 1697  
 1698  
 1699  
 1700  
 1701  
 1702  
 1703  
 1704  
 1705  
 1706  
 1707  
 1708  
 1709  
 1710  
 1711  
 1712  
 1713  
 1714  
 1715  
 1716  
 1717  
 1718  
 1719  
 1720  
 1721  
 1722  
 1723  
 1724  
 1725  
 1726  
 1727  
 1728  
 1729  
 1730  
 1731  
 1732  
 1733  
 1734  
 1735  
 1736  
 1737  
 1738  
 1739  
 1740  
 1741  
 1742  
 1743  
 1744  
 1745  
 1746  
 1747  
 1748  
 1749  
 1750  
 1751  
 1752  
 1753  
 1754  
 1755  
 1756  
 1757  
 1758  
 1759  
 1760  
 1761  
 1762  
 1763  
 1764  
 1765  
 1766  
 1767  
 1768  
 1769  
 1770  
 1771  
 1772  
 1773  
 1774  
 1775  
 1776  
 1777  
 1778  
 1779  
 1780  
 1781  
 1782  
 1783  
 1784  
 1785  
 1786  
 1787  
 1788  
 1789  
 1790  
 1791  
 1792  
 1793  
 1794  
 1795  
 1796  
 1797  
 1798  
 1799  
 1800  
 1801  
 1802  
 1803  
 1804  
 1805  
 1806  
 1807  
 1808  
 1809  
 1810  
 1811  
 1812  
 1813  
 1814  
 1815  
 1816  
 1817  
 1818  
 1819  
 1820  
 1821  
 1822  
 1823  
 1824  
 1825  
 1826  
 1827  
 1828  
 1829  
 1830  
 1831  
 1832  
 1833  
 1834  
 1835  
 1836  
 1837  
 1838  
 1839  
 1840  
 1841  
 1842  
 1843  
 1844  
 1845  
 1846  
 1847  
 1848  
 1849  
 1850  
 1851  
 1852  
 1853  
 1854  
 1855  
 1856  
 1857  
 1858  
 1859  
 1860  
 1861  
 1862  
 1863  
 1864  
 1865  
 1866  
 1867  
 1868  
 1869  
 1870  
 1871  
 1872  
 1873  
 1874  
 1875  
 1876  
 1877  
 1878  
 1879  
 1880  
 1881  
 1882  
 1883  
 1884  
 1885  
 1886  
 1887  
 1888  
 1889  
 1890  
 1891  
 1892  
 1893  
 1894  
 1895  
 1896  
 1897  
 1898  
 1899  
 1900  
 1901  
 1902  
 1903  
 1904  
 1905  
 1906  
 1907  
 1908  
 1909  
 1910  
 1911  
 1912  
 1913  
 1914  
 1915  
 1916  
 1917  
 1918  
 1919  
 1920  
 1921  
 1922  
 1923  
 1924  
 1925  
 1926  
 1927  
 1928  
 1929  
 1930  
 1931  
 1932  
 1933  
 1934  
 1935  
 1936  
 1937  
 1938  
 1939  
 1940  
 1941  
 1942  
 1943  
 1944  
 1945  
 1946  
 1947  
 1948  
 1949  
 1950  
 1951  
 1952  
 1953  
 1954  
 1955  
 1956  
 1957  
 1958  
 1959  
 1960  
 1961  
 1962  
 1963  
 1964  
 1965  
 1966  
 1967  
 1968  
 1969  
 1970  
 1971  
 1972  
 1973  
 1974  
 1975  
 1976  
 1977  
 1978  
 1979  
 1980  
 1981  
 1982  
 1983  
 1984  
 1985  
 1986  
 1987  
 1988  
 1989  
 1990  
 1991  
 1992  
 1993  
 1994  
 1995